

Implementation of Ln(AlMe₄)₃ as Precursors in Postlanthanidocene Chemistry

Melanie Zimmermann, Karl W. Törnroos, and Reiner Anwander*

Department of Chemistry, University of Bergen, Allégaten 41, N-5007, Bergen, Norway

Received March 17, 2006

cis-2,5-Bis[*N,N*-((2,6-diisopropylphenyl)amino)methyl]tetrahydrofuran (H₂BDPPthf) was obtained from LiNH(2,6-*i*-Pr₂C₆H₃) and *cis*-2,5-bis((tosyloxy)methyl)tetrahydrofuran in high yield and employed as a new [NON]²⁻ ancillary ligand for rare-earth metal centers. The reaction of H₂BDPPthf with homoleptic tetramethylaluminates Ln(AlMe₄)₃ (Ln = Y, Nd, La) quantitatively yielded heterobimetallic complexes (BDPPthf)Ln(AlMe₄)(AlMe₃) via alkane elimination. X-ray structure analysis of (BDPPthf)Ln(AlMe₄)(AlMe₃) (Ln = Y, La) revealed different coordination modes of BDPPthf, AlMe₄⁻, and AlMe₃. The yttrium derivative displays an η²-coordination of BDPPthf and insertion of AlMe₃ into one of the Ln–N anilido bonds to form a novel [Ln^{III}(μ-Me)₂AlMe(NR₂)] moiety. In contrast, BDPPthf coordinates the larger lanthanum center in an η³ fashion involving a heterobridging [La(μ-NR₂)(μ-Me)AlMe₂] moiety. The AlMe₄⁻ ligand adopts an unusual distorted μ:η³- (La) and a routine μ:η²-coordination mode (Y) depending on the size of the metal center. The intrinsic [NON]²⁻ ligand functionality for the first time implied the formation and structural identification of a kinetically favored aluminate/HR protonolysis product (Y), whereas the thermodynamically favored Ln–amido contact is found for the lanthanum derivative. All organolanthanide complexes were fully characterized by NMR and FTIR spectroscopy and elemental analysis.

Introduction

The quest for new, highly active and selective polymerization catalysts continues to stimulate research directed toward ancillary ligand and metal precursor design.¹ Recent developments in organolanthanide chemistry have focused on the use of non-cyclopentadienyl ancillary ligands, with much of the interest in “postlanthanidocene” chemistry being linked to the formation of cationic alkyl species.² In general, the activity and selectivity of a catalyst is related to precatalyst stability and the active species derived therefrom. To date, chelating diamido ligands of the type [NDoN]²⁻, such as [NNN]²⁻,³ [NON]²⁻,⁴ and [NPN]²⁻,⁵ have proved to be particularly useful in the formation of discrete and stable lanthanide complexes. In a previous study we reported the synthesis of a series of [NNN]LnR(THF)_x (Ln = Sc, Y, Lu; R = CH₂SiMe₃, N^{*i*}Pr₂, N(SiHMe₂)₂, NEt₂) complexes derived from H₂BDPPpyr (2,6-bis((2,6-diisopropylphenyl)amino)methyl)pyridine)^{3b} and the applicability of the scandium derivatives for the living polymerization of methyl methacrylate (MMA).

The successful complexation of such diamido ligands is limited by the availability of suitable precursors (namely, alkyl

species) for the entire lanthanide series.⁶ To date, Ln(CH₂-SiMe₃)₃(THF)_x (x = 2, 3),⁷ Ln[CH(SiMe₃)₂]₃,⁸ Ln(CH₂SiMe₂-Ph)₃(THF)₂,⁹ and Ln(*o*-Me₂NC₆H₄CH₂)₃¹⁰ represent the most commonly used lanthanide alkyl precursors that facilitate the formation of postlanthanidocene complexes via an alkane elimination reaction.

We have recently shown that homoleptic complexes Ln(AlMe₄)₃ (Ln = Y, La, Nd, Lu) are convenient synthetic precursors en route to mononuclear bis(tetraalkylaluminate) half-sandwich complexes of the type (C₅Me₅)Ln(AlMe₄)₂.¹¹ Herein, we describe the use of Ln(AlMe₄)₃ as precursors for the synthesis of postlanthanidocene complexes using *cis*-2,5-bis[*N,N*-((2,6-diisopropylphenyl)amino)methyl]tetrahydrofuran (H₂-BDPPthf, H₂[1]) as a new donor-functionalized diamido ligand.

Results and Discussion

[NDoN]²⁻ Ancillary Ligand Library. Our initial investigations into [NDoN]²⁻ diamido-based postlanthanidocene chemistry revealed an unexpected beneficial effect of an additional donor (Do) functionality in the ligand backbone.^{3b} While five-coordinate complexes [^{*i*}PrNNN^{*i*}Pr]ScR(THF) initiated the living polymerization of MMA, four-coordinate [^{*i*}PrNN^{*i*}Pr]ScR(THF), lacking a donor functionality, did not show any polymerization activity. We also found that the stability of complexes [^{*i*}PrNNN^{*i*}Pr]-

* Corresponding author. Fax: +47 555 89490. E-mail: reiner.anwander@kj.uib.no.

(1) (a) Schrock, R. R. *Acc. Chem. Res.* **1997**, *30*, 9. (b) Kempe, R. *Angew. Chem., Int. Ed.* **2000**, *39*, 468. (c) Gade, L. H. *Acc. Chem. Res.* **2002**, *35*, 575. (d) Piers, W. E.; Emslie, D. J. H. *Coord. Chem. Rev.* **2002**, *233–234*, 131. (e) Gibson, V. C.; Spitzmesser, S. K. *Chem. Rev.* **2003**, *103*, 283.

(2) Arndt, S.; Okuda, J. *Adv. Synth. Catal.* **2005**, *347*, 339.
(3) (a) Skinner, M. E. G.; Tyrell, B. R.; Ward, B. D.; Mountford, P. J. *Chem. Soc., Dalton Trans.* **2002**, 1694. (b) Estler, F.; Eickerling, G.; Herdtweck, E.; Anwander, R. *Organometallics* **2003**, *22*, 1212. (c) Sugiyama, H.; Korobkov, I.; Gambarotta, S.; Möller, A.; Budzelaar, P. H. M. *Inorg. Chem.* **2004**, *43*, 5771.

(4) Graf, D. D.; Davis, W. M.; Schrock, R. R. *Organometallics* **1998**, *17*, 5820.

(5) Fryzuk, M. D.; Yu, P.; Patrick, B. O. *Can. J. Chem.* **2001**, *79*, 1194.

(6) Bamber, S.; Bouwkamp, M. W.; Meetsma, A.; Hessen, B. J. *Am. Chem. Soc.* **2004**, *126*, 9182.

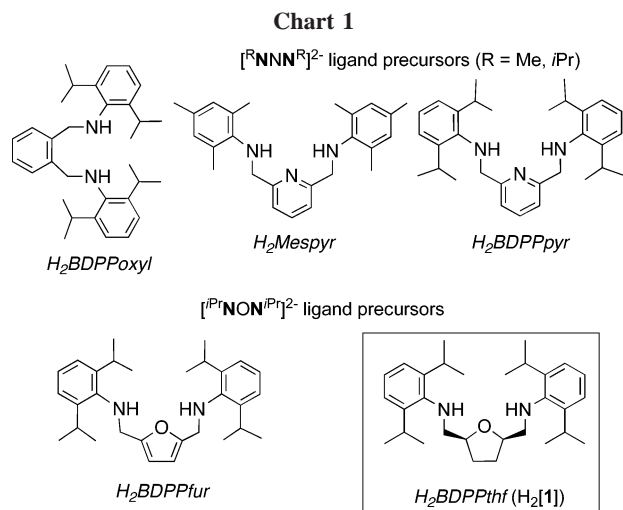
(7) Lappert, M. F.; Pearce, R. J. *Chem. Soc., Chem. Commun.* **1973**, 126.

(8) Hitchcock, P. B.; Lappert, M. F.; Smith, R. G.; Bartlett, R. A.; Power, P. P. *J. Chem. Soc., Chem. Commun.* **1988**, 1007.

(9) Emslie, D. J. H.; Piers, W. E.; Parvez, M.; McDonald, R. *Organometallics* **2002**, *21*, 4226.

(10) Harder, S. *Organometallics* **2005**, *24*, 373.

(11) Dietrich, H. M.; Zapilko, C.; Herdtweck, E.; Anwander, R. *Organometallics* **2005**, *24*, 5767.



$\text{LnR}(\text{THF})_x$ ($\text{Ln} = \text{Sc}$, $x = 1$; $\text{Ln} = \text{Lu}$, Y , $x = 2$) is governed by a metal size-dependent match/mismatch of the rigid tridentate ancillary ligand ($\text{Sc} \approx \text{Lu} \gg \text{Y}$) and by the steric shielding of the metal center via the ancillary ligand periphery ($[\text{^{*i*Pr}NNN^{*i*Pr}}] \gg [\text{^{Me}NNN^{Me}}]$). To get more insight into any structure–reactivity relations, we are currently attempting to complement this library by O-donor-functionalized ligands [^{*i*Pr}NON^{*i*Pr}]²⁻ as shown in Chart 1.

It can be anticipated that the complexation ability of rare-earth metal centers is markedly affected by (a) a smaller ring size in the ligand backbone, (b) an enhanced coordinative flexibility of the saturated tetrahydrofuran derivative, and (c) oxygen versus nitrogen donor coordination. While the “methyl” variant H_2BMPthf has previously been used for the synthesis of postzirconocene complex [^{Me}NON^{Me}] ZrMe_2 ,¹² $\text{H}_2\text{BDPPthf}$ and $\text{H}_2\text{BDPPfur}$ ¹³ appear to be new ligand precursors. $\text{H}_2\text{BDPPthf}$ ($\text{H}_2[1]$) was prepared in four steps from 5-hydroxymethylfuraldehyde following the manner reported by Flores et al.¹² In the last step of the synthesis *cis*-2,5-bis((tosyloxy)methyl)tetrahydrofuran was treated with $\text{LiNH}(2,6\text{-}i\text{Pr}_2\text{C}_6\text{H}_3)$ to yield diamine $\text{H}_2[1]$ as a white solid (93%). ¹H and ¹³C NMR spectra of $\text{H}_2[1]$ are in accordance with the *cis*-configuration of the molecule (mirror plane) and a highly flexible structure, as evidenced by rapid rotation of the aryl rings about the $\text{N}-\text{C}_{\text{ipso}}$ bond.

Synthesis and Characterization of Aluminato Complexes Derived from $\text{H}_2\text{BDPPthf}$ ($\text{H}_2[1]$). Compounds $(\text{BDPPthf})\text{-Ln}(\text{AlMe}_4)(\text{AlMe}_3)$ (Y , **3a**; La , **3b**; and Nd , **3c**) were prepared by slow addition of a hexane solution of $\text{Ln}(\text{AlMe}_4)_3$ to a solution of $\text{H}_2\text{BDPPthf}$ in hexane (Scheme 1).

The reaction was evidenced by instant gas evolution and the precipitation of **3** as analytically pure white solids for the yttrium and lanthanum derivative (**3a,b**) and as a blue-green solid for the neodymium compound (**3c**), respectively. The lanthanide complexes were obtained in nearly quantitative yields. In an attempt to examine the implications of the metal size for the complex formation, Y, Nd, and La were chosen as representative of smaller- and larger-sized rare-earth metal centers.

Single crystals of **3a** and **3b** suitable for X-ray structure analysis were grown from a hexane/toluene mixture (Figures 1

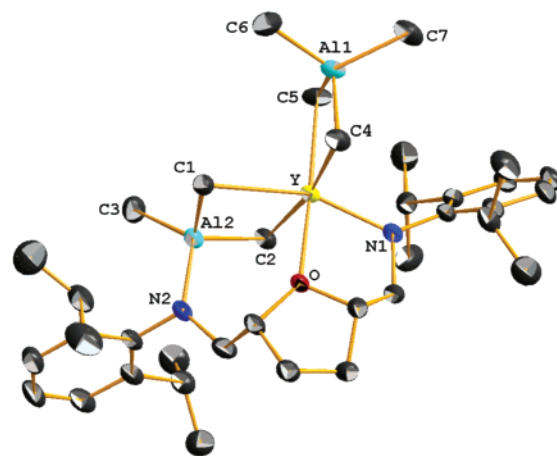


Figure 1. ORTEP drawing of $(\text{BDPPthf})\text{Y}(\text{AlMe}_4)(\text{AlMe}_3)$ (**3a**) in the solid state. Thermal ellipsoids are drawn at the 50% probability level. Hydrogen atoms are omitted for clarity. Atomic labels are given for selected atoms.

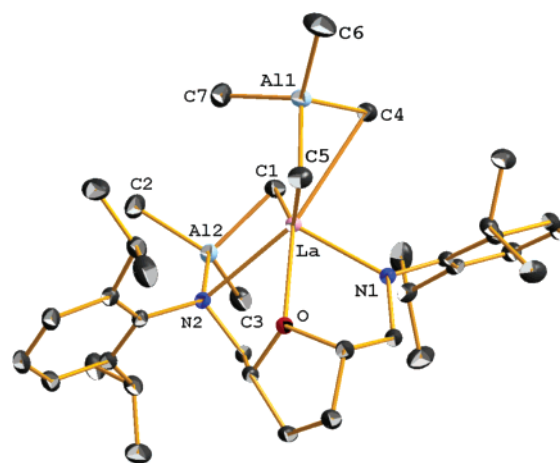
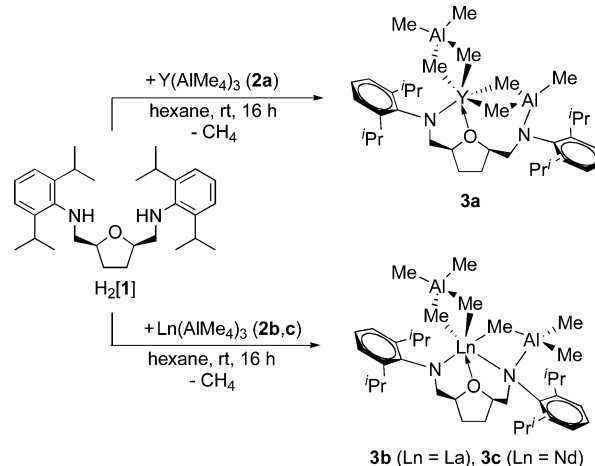


Figure 2. ORTEP drawing of $(\text{BDPPthf})\text{La}(\text{AlMe}_4)(\text{AlMe}_3)$ (**3b**) in the solid state. Thermal ellipsoids are drawn at the 50% probability level. Hydrogen atoms are omitted for clarity. Atomic labels are given for selected atoms.

Scheme 1. Synthesis of $(\text{BDPPthf})\text{Ln}(\text{AlMe}_4)(\text{AlMe}_3)$ ($\text{Ln} = \text{Y}$, La , and Nd) (3**) from $\text{H}_2\text{BDPPthf}$ (**1**) and $\text{Ln}(\text{AlMe}_4)_3$ ($\text{Ln} = \text{Y}$, La , and Nd) (**2**)**



(12) Flores, M. A.; Manzoni, M. R.; Baumann, R.; Davis, W. M.; Schrock, R. R. *Organometallics* **1999**, *18*, 3220.

(13) Zimmermann, M.; Herdtweck, E.; Anwender, R. Abstracts of Papers; 229th ACS National Meeting, San Diego, CA; American Chemical Society: Washington, DC, 2005; INOR 856.

and **2**). Selected bond distances and angles are listed in Table 1. Both complexes reveal the same net molecular composition of $(\text{BDPPthf})\text{Ln}(\text{AlMe}_4)(\text{AlMe}_3)$ with six-coordinate metal centers, however, a distinct organoaluminum coordination.

Table 1. Selected Interatomic Distances and Angles for (BDPPthf)Y(AlMe₄)(AlMe₃) (3a) and (BDPPthf)La(AlMe₄)(AlMe₃) (3b)

	3a (Ln = Y)	3b (Ln = La)
Bond Lengths (Å)		
Ln–N1	2.178(2)	2.333(2)
Ln–N2		2.817(2)
Ln–O	2.3376(15)	2.493(2)
Ln···Al1	3.0972(8)	3.0661(6)
Ln···Al2	3.1110(7)	3.3939(7)
Ln–C1	2.607(3)	2.696(2)
Ln–C2	2.584(3)	
Ln–C4	2.573(3)	2.920(2)
Ln–C5	2.516(3)	2.780(2)
Ln–C7		3.236(3)
Al1–C4	2.065(3)	2.055(3)
Al1–C5	2.072(3)	2.065(3)
Al1–C6	1.967(3)	1.958(3)
Al1–C7	1.960(3)	2.006(3)
Al2–N2	1.832(2)	1.951(2)
Al2–C1	2.062(3)	2.075(2)
Al2–C2	2.056(3)	1.971(3)
Al2–C3	1.958(3)	1.987(3)
Bond Angles (deg)		
N1–Ln–N2		109.5(1)
O–Ln–C5	176.7(1)	
O–Ln–N1	76.1(1)	69.3(1)
O–Ln–N2		67.5(1)
O–Ln–C1	81.9(1)	134.7(1)
O–Ln–C2	86.5(1)	
O–Ln–C4	95.0(1)	140.9(1)
N1–Ln–C1	158.0(1)	
N1–Ln–C2	96.3(1)	
N2–Ln–C1		72.8(1)
N2–Ln–C4		151.5(1)
N2–Ln–C5		127.7(1)
C4–Ln–C5	83.1(1)	71.2(1)
C4–Al1–C5	109.4(1)	107.4(1)
Ln–C4–Al1	83.0(1)	73.8(1)
Ln–C5–Al1	84.3(1)	76.9(1)
Ln–C1–Al2	82.7(1)	89.7(1)
Ln–C2–Al2	83.4(1)	
C1–Ln–C2	80.9(1)	
C1–Al2–C2	109.8(1)	

The yttrium complex **3a** adopts a distorted octahedral coordination geometry, with the Do-oxygen and one of the tetramethylaluminato carbons in the apical positions ($\angle\text{O–Y–C5} = 176.7^\circ$). The BDPPthf ancillary ligand is coordinated to the yttrium center in a η^2 fashion with very short Y–N1 (2.178(2) Å) and Y–O (2.338(2) Å) bond lengths. For comparison, the corresponding Y–[NON]^{2–} bond lengths in the five-coordinate complex [tBu-d₆-N-o-C₆H₄)₂O]Y[CH(SiMe₃)₂](THF) are 2.290 (av) and 2.337(8) Å.⁴ The AlMe₄[–] ligand coordinates in a η^2 fashion with an almost planar heterobimetallic [Y(μ -Me)₂Al] moiety ($\angle\text{C4–Y–C5–Al1} = -3.3^\circ$, interplanar angle C4YC5–C4Al1C5 = 5.7°). The Y–C bond lengths are in the expected range (Y–C1/C2 = 2.596 Å (av)).¹⁴ The AlMe₃ unit appears inserted into a fictitious Y–N2 bond, resulting in a novel [Ln^{III}(μ -Me)₂AlMe(NR₂)] moiety with slightly shortened Y–(μ -CH₃) bond lengths (Y–C4/C5 = 2.545 Å (av)). The [Y(μ -Me)₂Al] moiety is slightly bent toward the N2 atom ($\angle\text{C1–Y–C2–Al2} = -11.7^\circ$, interplanar angle C1YC2–C1Al2C2 = 20.4°). To the best of our knowledge Yb^{III}-[N(SiMe₃)₂]₂(AlMe₃)₂ is the only structure featuring a comparable [Ln(μ -Me)₂AlMe(NR₂)] unit.¹⁵

The lanthanum complex **3b** represents a rare example of a [NDoN]^{2–} postlanthanidocene complex with a large Ln(III)

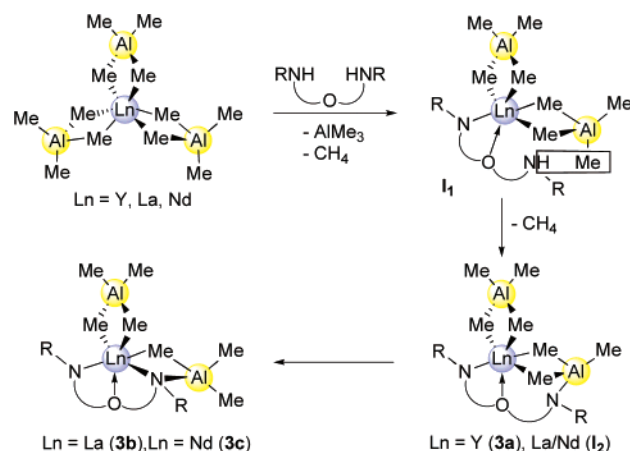
metal center.^{3,16} In contrast to yttrium complex **3a** the BDPPthf is coordinated to the lanthanum center in a η^3 fashion. One anilido nitrogen (N2) and one of the tetramethylaluminato methyl carbons (C4) occupy the apical positions of a strongly distorted octahedral coordination geometry ($\angle\text{N2–La–C4} = 151.5^\circ$). The two La–N bond lengths differ considerably due to the formation of one heterobridging [La(μ -NR₂)(μ -Me)Al] moiety, involving an extremely long La–N2 bond of 2.817(2) Å. For comparison, the bridging, terminal, and donor La–N bond distances in six-coordinate La[(μ -Me)₂GaMe₂][(μ-Me)-(μ-NMe₂)GaMe₂]₂¹⁷ and eight-coordinate (C₅Me₅)₂La(NHMe)-(H₂NMe)¹⁸ are 2.448 (av), 2.32(1), and 2.70(1) Å, respectively. Similar heterobridging moieties were described for Nd[NⁱPr₂]-[(μ -NⁱPr₂)(μ -Me)AlMe₂][(μ-Me)₂AlMe₂],¹⁹ [(Me₂Al(μ -Me)₂]₂Nd-(μ_3 -NC₆H₅)(μ -Me)AlMe₂]₂,²⁰ and [(μ -NC₆H₃ⁱPr₂-2,6)Sm(μ -NHC₆H₃ⁱPr₂-2,6)(μ -Me)AlMe₂]₂.²¹ The La–N1 bond of 2.333(2) Å is considerably shorter than those in six-coordinate La complexes supported by a diaminopyridine [NNN]^{2–}-type ligand (2.409 Å).^{3c} As with the yttrium compound **3a** a strong interaction of the donor in the ligand backbone with the metal center is indicated by a relatively short La–O bond length of 2.493(2) Å, cf. La–O in five-coordinate La[N(SiHMe₂)₂]₃-(THF)₂ of 2.564(4) and 2.583(4) Å.²²

The AlMe₄[–] ligand shows structural features similar to those recently found for (C₅Me₅)La(AlMe₄)₂.¹¹ It provides an atypically bent heterobimetallic [La(μ -Me)₂Al] moiety ($\angle\text{C4–La–C5–Al1} = -32.8^\circ$, interplanar angle C4LaC5–C4Al1C5 = 63.2°) with an additional La···(μ -CH₃) contact of 3.236(3) Å (La···C7), due to the steric unsaturation of the large lanthanum metal center. This pronounced La···C7 contact is also evidenced by differing bond angles $\angle\text{La–Al–C}_{\text{terminal}}$ of the bent ($\angle\text{La–Al1–C6/7} = 167.2^\circ$, 76.1°) compared to the η^2 -bonded aluminate ligands ($\angle\text{Y–Al1–C6/7} = 117.2^\circ$, 123.7°) of the analogous yttrium complex **3a**. Hence, the bent AlMe₄[–] ligand accomplishes a distorted η^3 coordination mode comparable to that in (C₅Me₅)La(AlMe₄)₂.¹¹ The other La–(μ -CH₃) bond lengths range from 2.695(2) to 2.920(2) Å, with the heterobridging moiety forming the shortest contact, cf., La–(μ -CH₃) in (C₅Me₅)La(AlMe₄)₂ of 2.694(3)–2.802(4) Å.¹¹

The ¹H NMR spectra of complexes **3a** and **3b** in C₆D₆ revealed a rigid coordination of the BDPPthf ligand at ambient temperature, indicating a large rotational barrier for the aryl groups around the N–C_{ipso} bond. The signals for the N-methylene protons (**3a**: 3.79 ppm; **3b**: 3.53 ppm) and the CH_{thf} (**3a**: 4.75, 4.65 ppm; **3b**: 4.82, 4.05 ppm) are shifted significantly downfield compared to H₂[1] (3.07 ppm res. 2.98 ppm). The isopropyl groups of the [NON]^{2–} ligand also exhibit two significantly downfield shifted multiplets for the methine groups (**3a**: 3.79, 3.48 ppm; **3b**: 3.76, 3.53 ppm) compared to H₂[1] (3.54 and 2.66 ppm), as well as four doublets for the methyl groups. The ¹H NMR spectrum of **3a** in C₆D₆ clearly revealed four signals in the alkyl region at 25 °C, suggesting enhanced fluxionality of the [AlMe₄] and [AlMe₃] moieties in solution (cf., seven methyl resonances would have been expected for an

(16) Izod, K.; Liddle, S. T.; Clegg, W. *Chem. Commun.* **2004**, 1748.(17) Evans, W. J.; Anwender, R.; Doedens, R. J.; Ziller, J. W. *Angew. Chem., Int. Ed. Engl.* **1994**, *33*, 1641.(18) Gagné, M. R.; Stern, C. L.; Marks, T. J. *J. Am. Chem. Soc.* **1992**, *114*, 275.(19) Evans, W. J.; Anwender, R.; Ziller, J. W. *Inorg. Chem.* **1995**, *34*, 5930.(20) Evans, W. J.; Ansari, M. A.; Ziller, J. W.; Khan, S. I. *Inorg. Chem.* **1996**, *35*, 5435.(21) Gordon, J. C.; Giesbrecht, G. R.; Clark, D. L.; Hay, P. J.; Keogh, D. W.; Poli, R.; Scott, B. L.; Watkin, J. G. *Organometallics* **2002**, *21*, 4726.(22) Anwender, R.; Runte, O.; Eppinger, J.; Gerstberger, G.; Herdtweck, E.; Spiegler, M. *J. Chem. Soc., Dalton Trans.* **1998**, 847.(14) Evans, W. J.; Anwender, R.; Ziller, J. W. *Organometallics* **1995**, *14*, 1107.(15) Boncella, J. M.; Anderson, R. A. *Organometallics* **1985**, *4*, 205.

Scheme 2. Kinetically versus Thermodynamically Controlled "Aluminate Elimination" Mediated by a Chelating Diamido Ligand



entirely nonfluxional arrangement, as proposed by the fully asymmetric solid-state structure). The terminal methyl groups of $[\text{AlMe}_4]$ show a broad singlet at -0.15 ppm at ambient temperature, whereas the signal for the bridging methyl groups can clearly be assigned by a characteristic doublet at -0.13 ppm ($^2J_{\text{Y,H}} = 2.4$ Hz). These resonances are shifted to lower field in comparison with the homoleptic precursor **2a** (-0.27 ppm). Various temperature NMR studies in toluene- d_8 support this assignment by coalescence of the $[\text{AlMe}_4]$ methyl resonances due to rapid exchange of bridging and terminal methyl groups at elevated temperatures. Two separate signals at 0.12 and -0.38 ppm (integral ratio 6:3) can be assigned to the $[\text{AlMe}_3]$ methyl groups. Curiously, the methyl group appearing at -0.38 ppm indicates an interaction with the yttrium center ($^2J_{\text{Y,H}} = 2.8$ Hz), which is opposed to the solid-state structure of **3a**, however would be more in favor of a methyl group arrangement as detected in the solid-state structure of **3b**. Coalescence of the $[\text{AlMe}_3]$ methyl resonances was not observed at elevated temperatures, consistent with an increased rigidity compared to **3b** due to enhanced steric crowding at the yttrium center. In contrast, the ^1H NMR spectrum of **3b** at 25°C showed only two signals in the methyl alkyl region. The signal at 0.01 ppm can be assigned to the $[\text{AlMe}_4]$ moiety and the signal at -0.05 ppm is the resonance of the $[\text{AlMe}_3]$ methyl groups. Both signals are shifted to lower field compared to the homoleptic precursor **2b** (-0.20 ppm), and the $[\text{La}(\mu\text{-Me})\text{AlMe}]$ moieties indicate a rapid exchange of bridging and terminal methyl groups. These results are consistent with an increased steric unsaturation at the larger lanthanum metal center. Elemental analysis, IR data, and a well-resolved ^{13}C NMR spectrum of paramagnetic **3c** clearly indicate the formation of complex $(\text{BDPPthf})\text{Nd}(\text{AlMe}_4)(\text{AlMe}_3)$. The size similarity of the neodymium and lanthanum metal centers suggests a solid-state structure of **3c** analogous to **3b**.

Based on the structural and dynamic features of complexes **3** a consecutive aluminate/diamido ligand exchange can be rationalized as shown in Scheme 2. Accordingly, the first amino functionality can easily approach the six-coordinate metal center of the homoleptic precursor via displacement of one AlMe_4^- ligand and formation of a strongly bonded $[\text{NO}]^-$ -chelating ligand, intermediate **I1**; this is also evidenced by the facile reaction of $\text{Ln}(\text{AlMe}_4)_3$ with donor molecules.²³ Subsequently, the dangling second amino group reacts with a terminal methyl

group of another AlMe_4^- ligand, affording the kinetically favored product **I2**. Such a derivative was isolated for Y as compound **3a**. Apparently, due to enhanced steric hindrance, the second amino functionality is unable to approach the smaller yttrium center to form a second thermodynamically favored Ln–amido contact, as found in the lanthanum derivative **3b**.

Conclusion

Homoleptic alkyl complexes $\text{Ln}(\text{AlMe}_4)_3$ display a high potential as precursors for postlanthanidocene chemistry. The new ancillary ligand precursor $\text{H}_2\text{BDPPthf}$ has been successfully employed for the preparation of the first postlanthanidocene complexes featuring both small and large Ln^{III} metal centers as well as tetramethylaluminate actor ligands. Moreover, the intrinsic $[\text{NON}]^{2-}$ ligand functionality for the first time implied the formation of a kinetically favored aluminate/HR protonolysis product and the identification of a $[\text{Ln}(\mu\text{-Me})_2\text{AlMe}(\text{NR}_2)]$ heterobimetallic moiety unprecedented in organolanthanide(III) chemistry. Complexes $(\text{BDPPthf})\text{Ln}(\text{AlMe}_4)(\text{AlMe}_3)$ are the subject of very promising reactivity and activity studies.

Experimental Details

General Procedures. All reactions and manipulations with air-sensitive compounds were performed under dry argon, using standard Schlenk and glovebox techniques (MB Braun MBLab; <1 ppm O_2 , <1 ppm H_2O). Hexane, THF, and toluene were purified by using Grubbs columns (MBraun SPS, solvent purification system). All solvents were stored in a glovebox. Deuterated solvents were degassed and dried over Na/K alloy and stored in a glovebox. Reagents were obtained from commercial suppliers and used without further purification, unless otherwise noted. Homoleptic $\text{Ln}(\text{AlMe}_4)_3$ ($\text{Ln} = \text{Y, La}$)¹⁴ and *cis*-2,5-bis((tosyloxy)methyl)-tetrahydrofuran¹² were synthesized according to the literature method. NMR spectra were recorded at 25°C on a Bruker-AVANCE-DMX400 (^1H : 400.13 MHz; ^{13}C : 100.62 MHz). ^1H and ^{13}C shifts are referenced to internal solvent resonances and reported in parts per million relative to TMS. IR spectra were recorded on a Nicolet-Impact 410 FTIR spectrometer as Nujol mulls sandwiched between CsI plates. Elemental analyses were performed on an Elementar Vario EL III, with samples that have been dried in vacuo.

***cis*-2,5-Bis[*N,N*-(2,6-diisopropylphenyl)amino)methyl]-tetrahydrofuran ($\text{H}_2\text{BDPPthf}$, $\text{H}_2[1]$).** A solution of lithium 2,6-diisopropylanilide (2.36 g, 12.98 mmol) in THF (15 mL) was added slowly to a stirred solution of *cis*-2,5-bis((tosyloxy)methyl)-tetrahydrofuran (2.86 g, 6.49 mmol) in THF (100 mL) at -78°C . The mixture was warmed to ambient temperature and stirred for 40 h, and all volatile components were then removed in vacuo. The residue was extracted with toluene (3×50 mL), and the extract was dried in vacuo. The product was purified by column chromatography (silica, pentane/ethyl acetate = 95/05 as eluent) to give $\text{H}_2[1]$ as a white solid (2.72 g, 6.03 mmol, 93%). IR (Nujol, cm^{-1}): 3387 m N–H, 1916 w, 1856 w, 1796 w, 1621 m, 1586 m, 1459 vs Nujol, 1377 vs Nujol, 1363 s, 1308 w, 1255 m, 1220 w, 1190 m, 1178 s, 1082 s, 1056 m, 946 w, 885 w, 851 w, 802 m, 755 s, 665 m, 621 w, 573 w, 555 w, 530 w, 430 w. ^1H NMR (400 MHz, C_6D_6 , 25°C): δ 7.14 (m, 6 H, ar), 3.98 (m, 2 H, CH_{thf}), 3.56 (s br, 2 H, N–H), 3.54 (sp, 4 H, ar–CH), 3.07 (dd, $^2J \cong 12.8$ Hz, $^3J \cong 4.0$ Hz, 2 H, N– CH_2), 2.98 (dd, $^2J \cong 12.8$ Hz, $^3J \cong 6.0$ Hz, 2 H, N– CH_2), 1.53 (m, 2 H, thf), 1.40 (m, 2 H, thf), 1.29 (d, $^3J \cong 6.0$ Hz, 24 H, CH_3). ^1H NMR (400 MHz, CDCl_3 , 25°C): δ 7.22 (m, 6 H, ar), 4.31 (m, 2 H, CH_{thf}), 3.50 (sp, 4 H, ar–CH), 3.47 (s br, 2 H, N–H), 3.18 (dd, $^2J \cong 12.4$ Hz, $^3J \cong 3.3$ Hz, 2 H, N– CH_2), 3.08 (dd, $^2J \cong 12.4$ Hz, $^3J \cong 7.7$ Hz, 2 H, N– CH_2), 2.17 (m, 2 H, thf), 1.91 (m, 2 H, thf), 1.42 (d, $^3J \cong 7.2$ Hz, 24 H, CH_3). ^{13}C NMR (100 MHz, CDCl_3 , 25°C): δ 142.5, 129.0, 122.7, 118.5 (C_{ar}),

(23) Dietrich, H. M.; Raudaschl-Sieber, G.; Anwander, R. *Angew. Chem. Int. Ed.* **2005**, *44*, 5303.

71.5 (C_{thf}), 56.3 (N-CH₂), 29.0 (C_{thf}), 27.6 (ar-CH), 24.3 (CH₃). Anal. Calcd for C₃₀H₄₆N₂O (450.706 g/mol): C, 79.95; H, 10.29; N, 6.22. Found: C, 80.28; H, 10.15; N, 6.07.

General Procedure for the Preparation of (BDPPthf)Ln-(AlMe₄)(AlMe₃), 3a–c. In a glovebox, Ln(AlMe₄)₃ (**2a–c**) was dissolved in 5 mL of hexane and added to a stirred solution of 1 equiv of H₂BDPPthf (H₂[1]) in 5 mL of hexane. Instant gas formation was observed. The reaction mixture was stirred another 12 h at ambient temperature while the formation of a precipitate was observed. The product was separated by centrifugation and washed three times with 3 mL of hexane to yield **3** as powdery solids in almost quantitative yields. The remaining solids were crystallized from a hexane/toluene solution at -35 °C to give colorless (**3a**, **3b**) or blue-green crystals (**3c**) in moderate yields suitable for X-ray diffraction.

(BDPPthf)Y(AlMe₄)(AlMe₃) (3a). Following the procedure described above, Y(AlMe₄)₃ (**2a**) (104 mg, 0.30 mmol) and H₂-BDPPthf (H₂[1]) (133 mg, 0.30 mmol) yielded **3a** (105 mg, 0.15 mmol, 50%) as colorless crystals. IR (Nujol, cm⁻¹): 1459 vs Nujol, 1377 vs Nujol, 1307 w, 1248 m, 1216 w, 1188 s, 1183 m, 1124 m, 1055 m, 1015 w, 930 w, 895 w, 858 w, 831 w, 801 w, 781 m, 763 w, 694 m, 651 w, 572 w, 542 w, 497 w, 470 w. ¹H NMR (400 MHz, C₆D₆, 25 °C): δ 7.23 (m, 3 H, ar), 7.19 (m, 3 H, ar), 4.75 (m, 1 H, CH_{thf}), 4.65 (m, 1 H, CH_{thf}), 3.79 (m, 5 H, N-CH₂, ar-CH), 3.48 (sp, 2 H, ar-CH), 2.84 (dd, ²J ≅ 12.4 Hz, ³J ≅ 8.9 Hz, 1 H, N-CH₂), 1.48 (d, ³J ≅ 6.8 Hz, 3 H, CH₃), 1.44 (d, ³J ≅ 6.8 Hz, 3 H, CH₃), 1.42 (d, ³J ≅ 7.2 Hz, 3 H, CH₃), 1.40 (d, ³J ≅ 7.2 Hz, 3 H, CH₃), 1.38 (d, ³J ≅ 7.2 Hz, 3 H, CH₃), 1.29 (d, ³J ≅ 7.2 Hz, 3 H, CH₃), 1.24 (d, ³J ≅ 6.8 Hz, 3 H, CH₃), 1.14 (d, ³J ≅ 6.8 Hz, 3 H, CH₃), 1.18 (m, 2 H, thf), 0.93 (m, 2 H, thf), 0.12 (s, 6 H, Al(CH₃)₃), -0.13 (d, ²J_{Y,H} ≅ 2.4 Hz, 6 H, Al(μ-CH₃)₂(CH₃)₂), -0.15 (s br, 6 H, Al(μ-CH₃)₂(CH₃)₂), -0.38 (d, ²J_{Y,H} ≅ 2.8 Hz, 3 H, Al(CH₃)₃). ¹³C NMR (100 MHz, C₆D₆, 25 °C): δ 151.0, 148.2, 147.1, 144.9, 144.7, 125.1, 124.8, 124.4, 124.1, 123.8 (C_{ar}), 88.2 (C_{thf}), 85.2 (C_{thf}), 65.0 (N-CH₂), 59.6 (N-CH₂), 31.8, 29.4, 28.5, 28.2, 27.4, 25.8, 25.6, 24.9, 24.5, 24.4, 24.1, 23.4 (C_{thf}, ar-CH, CH₃), 2.4 (s br, Al(CH₃)₄), 1.9 (s br, Al(CH₃)₄), 1.1 (s br, Al(CH₃)₃). Anal. Calcd for C₃₇H₆₅N₂OAl₂Y (696.804): C, 63.77; H, 9.40; N, 4.02. Found: C, 64.02; H, 9.27; N, 3.93.

(BDPPthf)La(AlMe₄)(AlMe₃) (3b). Following the procedure described above, La(AlMe₄)₃ (**2b**) (154 mg, 0.39 mmol) and H₂-BDPPthf (H₂[1]) (173 mg, 0.39 mmol) yielded **3b** (193 mg, 0.26 mmol, 66%) as colorless crystals. IR (Nujol, cm⁻¹): 1459 vs Nujol, 1377 vs Nujol, 1309 w, 1252 m, 1219 w, 1196 m, 1171 s, 1083 s, 1054 m, 961 w, 931 w, 892 w, 843 w, 799 m, 755 s, 696 m, 652 w, 564 w, 530 w, 513 w, 466 w. ¹H NMR (400 MHz, C₆D₆, 25 °C): δ 7.26 (m, 3 H, ar), 7.06 (m, 3 H, ar), 4.82 (m, 1 H, CH_{thf}), 4.05 (m, 1 H, CH_{thf}), 3.76 (m, 3 H, N-CH₂, ar-CH), 3.53 (m, 3 H, N-CH₂, ar-CH), 2.65 (dd, ²J ≅ 13.2 Hz, ³J ≅ 4.4 Hz, 1 H, N-CH₂), 2.27 (sp, 1 H, ar-CH), 1.58 (d, ³J ≅ 7.2 Hz, 3 H, CH₃), 1.55 (d, ³J ≅ 7.2 Hz, 3 H, CH₃), 1.47 (d, ³J ≅ 6.8 Hz, 3 H, CH₃), 1.40 (d, ³J ≅ 7.2 Hz, 3 H, CH₃), 1.38 (d, ³J ≅ 6.8 Hz, 3 H, CH₃), 1.34 (d, ³J ≅ 6.8 Hz, 3 H, CH₃), 1.31 (d, ³J ≅ 6.8 Hz, 3 H, CH₃), 1.20 (d, ³J ≅ 6.8 Hz, 3 H, CH₃), 1.15 (m, 2 H, thf), 0.99 (m, 2 H, thf), 0.01 (s, 12 H, Al(CH₃)₄), -0.05 (s, 9 H, Al(CH₃)₃). ¹³C NMR (100 MHz, C₆D₆, 25 °C): δ 149.9, 147.7, 147.3, 144.9, 144.2, 127.1, 125.4, 125.3, 125.1, 124.1 (C_{ar}), 86.6 (C_{thf}), 84.1 (C_{thf}), 65.6 (N-CH₂), 59.5 (N-CH₂), 33.5, 29.7, 28.4, 28.3, 28.2, 27.7, 26.8, 26.1, 25.6, 25.4, 24.9, 24.2, 24.0 (C_{thf}, ar-CH, CH₃), 2.3 (s br, Al(CH₃)₄), 2.0 (s br, Al(CH₃)₃). Anal. Calcd for C₃₇H₆₅N₂OAl₂La (746.633): C, 59.51; H, 8.77; N, 3.75. Found: C, 59.46; H, 8.68; N, 3.72.

(BDPPthf)Nd(AlMe₄)(AlMe₃) (3c). Following the procedure described above, Nd(AlMe₄)₃ (**2c**) (182 mg, 0.45 mmol) and H₂-BDPPthf (H₂[1]) (202 mg, 0.45 mmol) yielded **3c** (237 mg, 0.32 mmol, 70%) as blue-green crystals. IR (Nujol, cm⁻¹): 1459 vs Nujol, 1377 vs Nujol, 1313 w, 1302 s, 1253 m, 1236 s, 1222 w, 1189 m, 1172 s, 1146 w, 1097 s, 1054 s, 1033 w, 1003 w, 988 w,

Table 2. Crystal Data and Data Collection Parameters of Complexes 3a and 3b

	3a	3b
chem formula	C ₈₁ H ₁₃₈ N ₄ O ₂ Al ₄ Y ₂	C ₃₇ H ₆₅ N ₂ OAl ₂ La
fw	1485.69	746.78
color/shape	colorless/prism	colorless/needle
cryst size (mm)	0.35 × 0.18 × 0.13	0.38 × 0.90 × 0.07
cryst syst	triclinic	monoclinic
space group	<i>P</i> $\bar{1}$ (no. 2)	<i>P</i> ₂ / <i>n</i> (no. 14)
<i>a</i> (Å)	12.4487(6)	9.5128(7)
<i>b</i> (Å)	12.4523(6)	10.8146(8)
<i>c</i> (Å)	14.9992(7)	40.644(3)
α (deg)	106.758(1)	
β (deg)	90.620(1)	93.035(1)
γ (deg)	106.356(1)	
<i>V</i> (Å ³)	2125.51(18)	4175.5(5)
<i>Z</i>	2	4
<i>T</i> (K)	153(2)	153(2)
ρ _{calcd} (g cm ⁻³)	1.161	1.188
μ (mm ⁻¹)	1.443	1.092
<i>F</i> ₀₀₀	798	1568
θ range (deg)	2.08–26.37	2.01–30.03
data collected (<i>h</i> , <i>k</i> , <i>l</i>)	15, 15, 18	13, 15, 57
no. of reflns collected	27 908	70 529
no. of indep reflns/ <i>R</i> _{int}	8704 (all)/0.029	12 204 (all)/0.035
no. of obsd reflns (<i>I</i> > 2σ(<i>I</i>))	7496 (obsd)	10524 (obsd)
no. of params refined	439	403
<i>R</i> ₁ (obsd/all) ^a	0.0344/0.0447	0.0297/0.0373
w <i>R</i> ₂ (obsd/all) ^a	0.0900/0.0955	0.0672/0.0691
GOF (obsd/all) ^a	1.039/1.173	1.075/1.075
largest diff peak and hole (e Å ⁻³)	+0.498/-0.541	+0.507/-1.731

$$^a R_1 = (|F_o| - |F_c|)/|F_o|; wR_2 = \{[w(F_o^2 - F_c^2)^2]/w(F_o^2)^2\}^{1/2}; \text{GOF} = \{[w(F_o^2 - F_c^2)^2]/(n - p)\}^{1/2}.$$

933 w, 923 w, 891 w, 850 w, 833 w, 799 m, 787 m, 769 s, 721 m, 704 w, 560 w, 532 w, 509 w, 462 w. ¹H NMR (600 MHz, C₆D₆, 25 °C): δ 17.52, 17.10, 16.18, 13.17, 12.04, 10.67, 10.20, 10.00, 9.71, 7.03, 7.69, 5.93, 2.11, 2.08, 1.28, 1.08, 0.89, -2.84, -3.69, -4.75, -5.16, -9.88, -11.21, -11.79, -14.96, -16.45. ¹³C NMR (100 MHz, C₆D₆, 25 °C): δ 168.3, 154.5, 144.6, 142.8, 136.4, 129.3, 129.2, 125.5, 124.8 (C_{ar}), 76.0 (C_{thf}), 50.2 (N-CH₂), 41.8, 36.2, 35.4, 31.9, 30.1, 24.5, 22.2, 20.2, 16.7, 15.4 (C_{thf}, ar-CH, CH₃). Anal. Calcd for C₃₇H₆₅N₂OAl₂Nd (752.138): C, 59.09; H, 8.71; N, 3.72. Found: C, 58.92; H, 8.69; N, 3.71.

X-ray Crystallography and Crystal Structure Determination of 3a and 3b. Crystals suitable for diffraction experiments were selected in a glovebox and mounted in Paratone-N inside a nylon loop (Hampton research). Data collection was done on a Bruker AXS SMART 2K CCD diffractometer using graphite-monochromated Mo Kα radiation (λ = 0.71073 Å) performing ω-scans in four φ positions, employing the SMART software package.²⁴ A total of 1888 collected images were processed using SAINT.²⁵ Numerical absorption correction was done using SHELXTL.²⁶ The structures were solved by direct methods and refined with standard difference Fourier techniques.²⁶ The structure of **3a** contains a rotationally disordered toluene molecule lying on an inversion center. This molecule was refined with a 6-fold disorder model using SHELXL command DFIX to constrain the methyl to ring atom C–C distances to 1.52 Å. The FLAT command was applied to the ring atoms. The C atoms in the ring were refined anisotropically. The H atom positions of the AlMe groups are clearly visible in the difference Fourier map. The structure of **3b** contained one heavily disordered solvent molecule (hexane) that could not be

(24) SMART v. 5.054, Data Collection Software for Bruker AXS CCD; Bruker AXS Inc.: Madison, WI, 1999.

(25) SAINT v. 6.45a, Data Integration Software for Bruker AXS CCD; Bruker AXS Inc.: Madison, WI, 2002.

(26) SHELXTL v. 6.14, Structure Determination Software Suite; Bruker AXS Inc.: Madison, WI, 2000.

modeled, and it was therefore subtracted from the intensity data using the routine SQUEEZE as implemented in the program PLATON.²⁷ The subtracted contribution to the total scattering equals 54 electrons. After subtraction PLATON reported a solvent accessible volume of 204 Å³. In both **3a** and **3b**, the H atom positions of the AlMe groups are clearly visible in the difference Fourier map. All H atoms in the structure were geometrically positioned (AFIX 13, 43, 23, and 137) and their U_{iso} constrained to be between 1.2 and 1.5 times that of the parent atom. For further experimental details see Table 2. Crystallographic data (excluding structure factors) for the structures reported in this paper have been deposited with the Cambridge Crystallographic Data Centre as supplementary publication nos. CCDC-292070 (**3a**) and CCDC-292071 (**3b**). Copies of the data can be obtained free of charge on

application to CCDC, 12 Union Road, Cambridge CB2 1EZ, UK (fax: (+44)1223-336-033; e-mail: deposit@ccdc.cam.ac.uk).

Acknowledgment. We thank the Deutsche Forschungsgemeinschaft (SPP 1166), the Fonds der Chemischen Industrie, and the Bayerische Forschungsförderung for generous support. R.A. thanks Warren Piers and Joe Takats for stimulating discussions.

Supporting Information Available: Text giving tables of atomic coordinates, atomic displacement parameters, and bond distances and angles for complexes **3a** and **3b**. This material is available free of charge via the Internet at <http://pubs.acs.org>.

(27) Spek, A. L. *Acta Crystallogr., Sect. A* **1990**, *46*, C34.

OM060244D